False bifurcations in chemical systems: canards

By Bo Peng, Vilmos Gáspár† and Kenneth Showalter

Department of Chemistry, West Virginia University, Morgantown, West Virginia 26506-6045, U.S.A.

A canard is a false bifurcation in which the amplitude of an oscillatory system may change by orders of magnitude while the qualitative dynamical features remain unchanged. Recent theoretical considerations suggest that canards are characteristic of fast–slow dynamical systems and are associated with the stable and unstable manifolds of the phase plane. An alternative characterization of canard behaviour is proposed involving the crossing of an *inflection line* by a limit cycle growing out from an unstable stationary state. The inflection line comprises the locus of points at which the curvature of any phase plane trajectory is zero. The role of the inflection line in the onset of canard behaviour as well as in the continuity of the transition is examined in a two-variable model for the oscillatory EOE reaction, the Autocatalator, and the two-variable Oregonator. The approach is also applied to the van der Pol oscillator, the system in which canard behaviour was first examined.

1. Introduction

A canard is associated with a dramatic change in the period and amplitude of an oscillatory system within a very narrow range of the control parameter. Because the qualitative dynamical features remain unchanged during the transition, it is a *false* bifurcation: limit cycle oscillations occur before and after the canard. The transformation of small-amplitude, high-frequency limit cycle oscillations to large-amplitude, low-frequency ones occurs without a significant change in the vector field. For example, the character as well as the number of steady states in the phase space remain unchanged as a system passes through a canard.

Benoit *et al.* (1981) were first to characterize canards in an investigation of oscillation amplitude of the van der Pol system. (The term *canard* technically refers to middle-amplitude limit cycle solutions exhibited during the transition; here, it will be used interchangeably with *canard transition*.) Diener & Poston (1981) and Diener (1984) subsequently pointed out that canard behaviour is a general feature of fast–slow dynamical systems. A canard cycle, the middle-sized limit cycle solution, closely follows the stable part of the slow manifold (defined by the nullcline of the fast variable); on passing the knee of the S shaped nullcline, however, it continues to remain in the neighbourhood of the slow manifold, which is now unstable. Kaas-Petersen & Brons (1985) showed that this unusual sequence is due to two manifolds associated with the slow manifold: M_s, the stable (attracting) manifold and M_u, the unstable (repelling) manifold. The relative positions of the stable and unstable manifolds with respect to the knee of the slow manifold determine whether small- or large-amplitude oscillations occur. The *canard point* can be defined as the critical

† Permanent address: Department of Physical Chemistry, Kossuth Lajos University, 4010 Debrecen, P.O. Box 7, Hungary.

Phil. Trans. R. Soc. Lond. A (1991) **337**, 275–289
Printed in Great Britain

value of the control parameter at which the stable and unstable manifolds merge as one, the *canard manifold*.

Canard behaviour has also been reported in simple models for chemical oscillations, for example, in different modifications of the Autocatalator (Merkin *et al.* 1986, 1987; Gray *et al.* 1988; Scott & Tomlin 1990) and in a two-variable Oregonator (Bar-Eli & Brons 1991). The characterization of canard transitions in the Oregonator by Bar-Eli & Brons followed the theory of Kaas-Petersen & Brons (1985). They also showed that the same interplay of stable and unstable manifolds accounts for excitability exhibited by the Oregonator (Bar-Eli & Noyes 1987).

Canard behaviour has also been found in a two-variable model of the oscillatory iodate–sulphite–ferrocyanide reaction (Gáspár & Showalter 1990), discussed in §2. A characterization involving the interplay of stable and unstable manifolds proves to be inappropriate in this case, thus providing motivation for an alternate approach to characterize canards, presented in §3. By using the new approach, canard behaviour in the two-variable iodate–sulphite–ferrocyanide model is analysed in §4. The same approach is followed in analyses of the Autocatalator in §5 and the two-variable Oregonator in §6. In the latter, canard behaviour of an unstable limit cycle is characterized. Canard behaviour is revisited in the classic but non-chemical van der Pol system in §7, and application of the approach is summarized in §8.

2. Canard behaviour in a two-variable model of the Edblom–Orbán–Epstein (EOE) reaction

The first oscillatory chemical system based on the classic iodate–sulphite clock reaction (Landolt 1886) was discovered by Edblom *et al.* (1986). They found that the Landolt reaction becomes oscillatory in a continuous-flow, stirred tank reactor when ferrocyanide is added to the reactant stream. (This system is referred to as the oscillatory EOE reaction.) A ten-variable, empirical-rate-law model based on component processes proposed by Edblom *et al.* (1986) describes the detailed chemistry of the oscillatory reaction (Gáspár & Showalter 1987). This model was subsequently reduced to a four-variable description (Gáspár & Showalter 1990), which retained essentially all of the dynamical features found in experiments (Edblom *et al.* 1986; Gáspár & Showalter 1987). The four-variable model was further reduced to a minimal two-variable scheme. Transitions from steady state to oscillatory behaviour were investigated in the minimal model, revealing a saddle-loop bifurcation and canard behaviour associated with a supercritical Hopf bifurcation.

The four-variable model comprises one reversible and four irreversible steps (Gáspár & Showalter 1990):

$$\mathrm{A}+\mathrm{Y}\rightleftharpoons\mathrm{X}, \qquad [2.1]$$

$$\mathrm{X}\rightarrow\mathrm{Y}, \qquad [2.2]$$

$$2\mathrm{Y}\rightarrow\mathrm{Z}, \qquad [2.3]$$

$$\mathrm{Z}+\mathrm{X}\rightarrow3\mathrm{Y}, \qquad [2.4]$$

$$\mathrm{Z}\rightarrow. \qquad [2.5]$$

The variables and corresponding species of the chemical reactions are $\mathrm{A}\equiv\mathrm{SO}_3^{2-}$, $\mathrm{X}\equiv\mathrm{HSO}_3^-$, $\mathrm{Y}\equiv\mathrm{H}^+$ and $\mathrm{Z}\equiv\mathrm{I}_2$. A singular perturbation analysis of the associated system of differential equations allows the number of independent variables to be

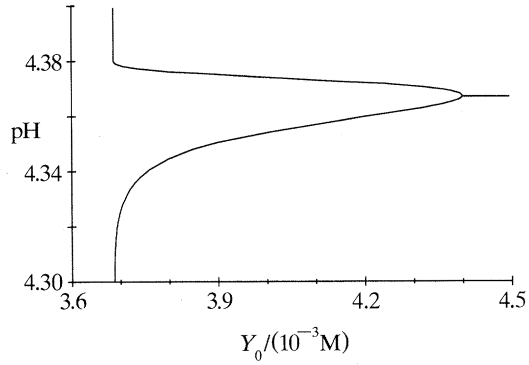

Figure 1. Transition from steady-state to oscillatory behaviour in the two-variable model for the oscillatory EOE reaction. Supercritical Hopf bifurcation occurs at critical input concentration $Y_0^* \approx 4.40 \times 10^{-3}$ M; vertical lines at $Y_0 \approx 3.68 \times 10^{-3}$ M show onset of canard transition. Amplitude of oscillations and steady-state pH calculated using the Livermore Solver of Ordinary Differential Equations (Gear 1971; Hindmarsh 1980). Values of rate constants and parameters: $k_1 = 5.0 \times 10^{10}$ M^{-1} s^{-1}, $k_{-1} = 8.1 \times 10^3$ s^{-1}, $k_2 = 6.0 \times 10^{-2}$ s^{-1}, $k_3 = 7.5 \times 10^4$ M^{-1}, $k_4 = 2.3 \times 10^9$ M^{-1} s^{-1}, $k_5 = 3.0 \times 10^1$ s^{-1}, $k_0 = 1.5 \times 10^{-3}$ s^{-1}, $A_0 = 9.0 \times 10^{-2}$ M.

reduced by eliminating the two fastest variables, A and Z. The result is a minimal two-variable system:

$$\mathrm{d}X/\mathrm{d}t = k_1 A_\mathrm{s} Y - (k_{-1} + k_2 + k_4 Z_\mathrm{s} + k_0) X, \tag{A 1}$$

$$\mathrm{d}Y/\mathrm{d}t = -k_1 A_\mathrm{s} Y + (k_{-1} + k_2 + 3k_4 Z_\mathrm{s}) X - 2k_3 Y^2 + k_0 (Y_0 - Y), \tag{A 2}$$

where A_s and Z_s are functions of X and Y,

$$A_\mathrm{s} = \frac{k_{-1} X + k_0 A_0}{k_1 Y + k_0}, \tag{A 3}$$

$$Z_\mathrm{s} = \frac{k_3 Y^2}{k_4 X + k_5 + k_0}. \tag{A 4}$$

The rate constant k_0 is the reciprocal residence time of the reactor (flow rate/volume), and A_0 and Y_0 represent the inflow concentrations of A and Y.

Figure 1 shows a supercritical Hopf bifurcation and associated canard behaviour in the two-variable model as the acidity of the reactant stream is varied. For comparison with earlier experimental and computational results (Gáspár & Showalter 1987, 1990), the stationary state pH and maximum and minimum of the pH oscillations are plotted. Small-amplitude oscillations emerge on decreasing the value of Y_0 below the critical Hopf value, $Y_0^* \approx 4.40 \times 10^{-3}$ M. The amplitude grows smoothly until $Y_0 \approx 3.68 \times 10^{-3}$ M, where there is a sharp increase resulting in large-amplitude oscillations ranging between pH 2.5 and 10.0 (see figure 2*a*). The transformation of the small-amplitude oscillations to large-amplitude relaxation oscillations occurs virtually discontinuously on variation of the bifurcation parameter. The transition was located with a resolution of 10^{-8} M in the value of Y_0; however, middle-amplitude oscillations ranging over eight orders of magnitude could not be resolved. Further increasing the resolution in Y_0 resulted in spurious solutions; the middle-amplitude solutions could not be found and, in fact, seem to be missing. The vertical lines in figure 1 therefore do not imply the existence of middle-size solutions, but rather indicate an apparent discontinuous jump in amplitude at the canard. We return to this dynamical feature in §4.

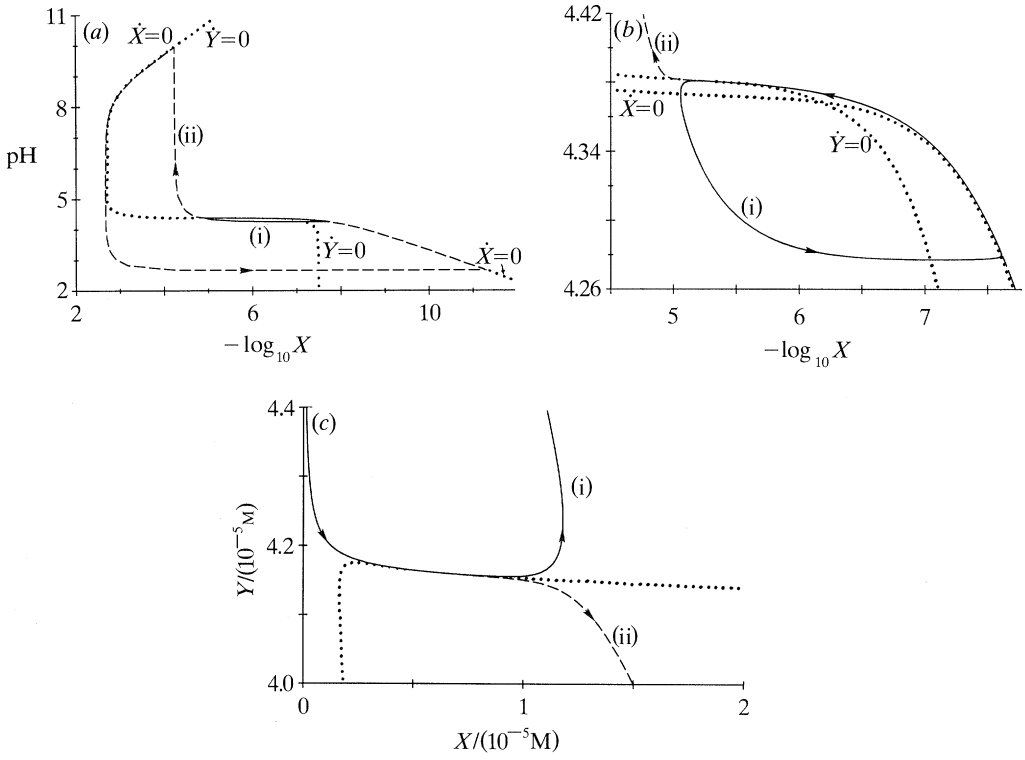

Figure 2. (*a*) Phase plane of two-variable model for the oscillatory EOE reaction showing limit cycles for small-amplitude (——, (i)) and large amplitude oscillations (– – –, (ii)), immediately before and after the canard transition. The corresponding values of the bifurcation parameter are $Y_0^{\mathrm{i}} = 3.685\,671 \times 10^{-3}$ M and $Y_0^{\mathrm{ii}} = 3.685\,669 \times 10^{-3}$ M. Two nullclines calculated at the intermediate value $Y_0^{\mathrm{nul}} = 3.685\,670 \times 10^{-3}$ M are shown by dotted lines. (*b*) Enlarged region of the phase plane shown in (*a*). (*c*) Further enlargement of phase plane with the inflection line (calculated at Y_0^{b}) shown by the dotted curve.

Figure 2*a* shows small and large limit cycles calculated at slightly different values of Y_0. Also shown in the figure are the nullclines, depicted by dotted lines. The extremely small variation in the value of Y_0 for the two limit cycles does not result in a detectable change in the nullclines; therefore, the average of the Y_0 values was used in determining their location (by the binary bisection method). Although the nullclines seem to run together in the upper part of the phase plane, an enlargement reveals that the Y-nullcline lies slightly to the right of the X-nullcline.

Figure 2*a* and the enlargement in figure 2*b* show that the large limit cycle follows the X-nullcline at low pH values and the Y-nullcline at high pH values. This feature indicates that the two-variable model of the EOE reaction is not a typical fast–slow variable system. Moreover, in the region where the small limit cycle encircles the steady state, shown in figure 2*b*, no extrema are exhibited in either of the nullclines. Consequently, a theoretical approach based on the interplay between stable and unstable manifolds cannot be applied in analysing this system.

Figure 2*b* indicates that both limit cycles follow a seemingly common path before they suddenly depart. There is, however, an important qualitative difference in the trajectories: a change in sign of the curvature occurs in the large limit cycle, while no such change is observed in the small limit cycle. In the following section we show

how changes in sign of the curvature of the trajectories define an important feature of the phase plane, the inflection line, which, in turn, leads to an alternative approach for understanding canard behaviour. We return to canard behaviour in the EOE reaction in §4.

3. The inflection line

Consider the ordinary differential equations for a general two-variable system:

$$\mathrm{d}X/\mathrm{d}t = \boldsymbol{f}(X, Y), \tag{1a}$$

$$\mathrm{d}Y/\mathrm{d}t = \boldsymbol{g}(X, Y). \tag{1b}$$

For any particular functions $\boldsymbol{f}$ and $\boldsymbol{g}$, equations (1) define a set of trajectories, fully occupying the XY phase plane. Of course, the evolution of the system is confined to a particular trajectory for any given initial conditions. Along such a phase path, the value of one dynamical variable can always be expressed as a unique function of the other, with time becoming an implicit variable (Andronov *et al.* 1966).

In the case of the two-variable EOE model, the canard transition is associated with a change in sign of the curvature of the limit cycle trajectory (figure 2*b*). In general, the curvature κ of a phase plane trajectory is defined as the rate of turn of the tangent with respect to the arc length s along the trajectory (Korn & Korn 1961). The curvature can easily be calculated from the first and second derivatives of Y with respect to X:

$$\kappa = \mathrm{d}\vartheta/\mathrm{d}s = (\mathrm{d}^2Y/\mathrm{d}X^2)/_+(1+(\mathrm{d}Y/\mathrm{d}X)^2)^{\frac{3}{2}}. \tag{2}$$

Choosing a direction, say the positive Y axis, defines a given trajectory as *concave* or *convex* if the second derivative (and thus curvature κ) is positive or negative respectively. This sign convention is used here in characterizing the curvature of a trajectory. Corresponding X and Y values that satisfy $\kappa = 0$ in (2) define the inflection line in the phase plane. Trajectories passing through this line (defining zero curvature) undergo a change in curvature from concave to convex or *vice versa*; i.e. the crossing point is an inflection point.

Consider a limit cycle formed at a supercritical Hopf bifurcation. The closed trajectory increases in size as the bifurcation parameter is varied, growing out approximately parabolically from the stationary state. At the same time, the inflection line also changes its position in the phase plane in a smooth and continuous manner. The growing limit cycle and inflection line may or may not touch as the bifurcation parameter is changed. If they do, the limit cycle trajectory asymptotically approaches a tangent to the inflection line. On crossing, it then diverges away with opposite curvature. The result is a sudden change in the size of the limit cycle, giving rise to canard behaviour. The critical value of the bifurcation parameter at which the limit cycle and the inflection line first touch is defined as the canard point.

It is important to point out that canard behaviour is associated with the first crossing of the inflection line by a limit cycle trajectory. Since a newly formed periodic orbit is approximately circular, the first crossing must occur tangentially and, thereby, result in a fundamental alteration of size and shape. Of course, crossings of the inflection line by a limit cycle must occur in pairs; therefore, the first crossing is always associated with another crossing at some other point on the limit cycle.

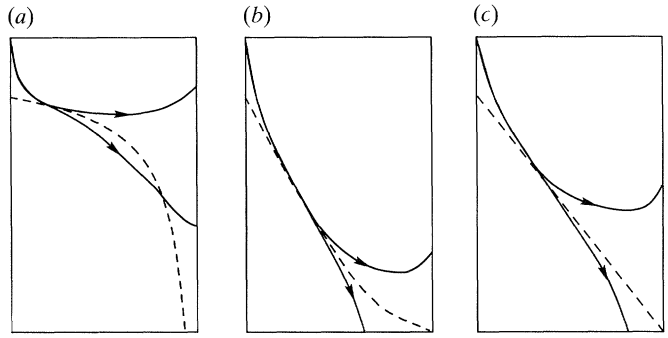

Figure 3. Relative curvatures of limit cycle trajectory and inflection line after first crossing. Limit cycle trajectory before crossing also shown for comparison. (*a*) Curvatures of inflection line (– –) and limit cycle trajectory (——) are of same sign beyond first crossing. (*b*) Curvatures are of opposite sign. (*c*) Limit cycle trajectory crossing a straight inflection line.

This characterization of canard behaviour does not require a special structure of nullclines in the phase plane. Whether or not a scheme results in a typical fast–slow dynamical system, canard behaviour is always associated with the crossing of an inflection line by an expanding limit cycle. Moreover, the continuity of a canard transition can be ascertained by comparing the curvature of the inflection line itself (κ_i) with that of the trajectory (κ_t) beyond the crossing point. To illustrate this point, three cases in which the limit cycle trajectory is convex ($\kappa_t < 0$) after the crossing are described. (An analogous argument can be made when the limit cycle is concave after the crossing.) A key element in the argument is that crossings must occur in pairs.

(*a*) For the configuration in figure 3*a*, κ_i and κ_t have the same sign (both curves are convex) after the crossing point, and the limit cycle trajectory soon recrosses the inflection line. The distance between the first and second crossings varies smoothly with the bifurcation parameter; in principle, the trajectory may recross the inflection line arbitrarily close to the first crossing point. This canard transition is therefore continuous.

(*b*) If the inflection line is concave ($\kappa_i > 0$) after the crossing point, as in figure 3*b*, the convex trajectory cannot recross arbitrarily close to the first crossing point. Now, as the bifurcation parameter is varied, the limit cycle trajectory diverges away from its original course after first touching the inflection line. The canard transition in this case is therefore discontinuous.

(*c*) When the inflection line is straight after the crossing point, as in figure 3*c*, the situation is analogous to case (*b*): the canard is discontinuous.

It should be noted that the effect of a discontinuous jump in amplitude, as in case (*b*) or (*c*), may be small since the second crossing can occur close to the first.

No canard behaviour is exhibited if a growing limit cycle does not intersect an inflection line in the phase plane. This may happen if the inflection line lies too far away from the stationary state undergoing Hopf bifurcation or if additional bifurcations take place before the growing limit cycle can touch the inflection line. The inflection line may also drift away from a growing limit cycle, thereby preventing a crossing. An example of a limit cycle expanding without canard behaviour is described in §5.

4. Canard behaviour in the two-variable model of the EOE reaction

The region of the phase plane depicted in figure 2*b* is enlarged in figure 2*c* with the inflection line indicated by the dotted curve. The locus of points making up the inflection line was determined with the value of Y_0 used for the large limit cycle (see Appendix A for equation used in bisection method calculation); a calculation with the value of Y_0 for the small limit cycle yields a line indistinguishable from that shown in the figure. On decreasing Y_0, the small limit cycle grows to become tangent with the inflection line; any further decrease results in the trajectory crossing the line and diverging away to trace out the larger limit cycle. The inflection line after the crossing point (to the right) bends slightly upward. Since κ_i and κ_t are of opposite sign beyond the crossing point, the canard transition is discontinuous (case *b*), explaining why the middle-amplitude solutions were missing in the numerical study.

A feature relevant to the existence of canard behaviour in the EOE reaction is the plateau behaviour found in the experimental and modelling studies. The calculated large-amplitude oscillations are interrupted by a short plateau at pH $\approx$ 4.38, coinciding with the inflection line crossing. Although small-amplitude oscillations associated with a Hopf–canard transition have not been found in experimental studies (Edblom *et al.* 1986; Gáspár & Showalter 1987), plateau behaviour is consistently observed at pH $\approx$ 4.25, indicating that the sudden onset of large-amplitude oscillations occurs via a canard transition. The canard possibly occurs too close to the Hopf bifurcation in the experimental system for the small-amplitude oscillations to be resolved. This explanation is consistent with the experimentally observed noisy fluctuations close to the transition to oscillatory behaviour (Gáspár & Showalter 1987). In other studies of experimental systems, the sudden appearance of large-amplitude oscillations has usually been attributed to subcritical Hopf bifurcations. The analysis of the EOE reaction shows that the sudden onset of large-amplitude oscillations may also occur via a supercritical Hopf bifurcation and associated canard transition.

5. Canard behaviour in the two-variable Autocatalator

In 1986 Gray & Scott proposed a simple scheme called the Autocatalator as a prototype for oscillatory behaviour in isothermal chemical systems. The two-variable scheme, in which canard behaviour has also been found (Merkin *et al.* 1986, 1987; Gray *et al.* 1988; Scott & Tomlin 1990), is related to the minimal model of the EOE reaction discussed above. The Autocatalator is comprised of four irreversible steps:

$$\mathrm{P} \rightarrow \mathrm{A}, \qquad [5.1]$$

$$\mathrm{A} \rightarrow \mathrm{B}, \qquad [5.2]$$

$$\mathrm{A} + 2\mathrm{B} \rightarrow 3\mathrm{B}, \qquad [5.3]$$

$$\mathrm{B} \rightarrow \mathrm{C}. \qquad [5.4]$$

The decay of precursor P to generate A is assumed to occur very slowly, allowing its concentration to be considered constant. Introducing a dimensionless time scale $\tau = k_2 t$ and the dimensionless variables $\alpha = (k_2/k_4)(k_3/k_2)^{\frac{1}{2}}A$ and $\beta = (k_3/k_2)^{\frac{1}{2}}B$ for the

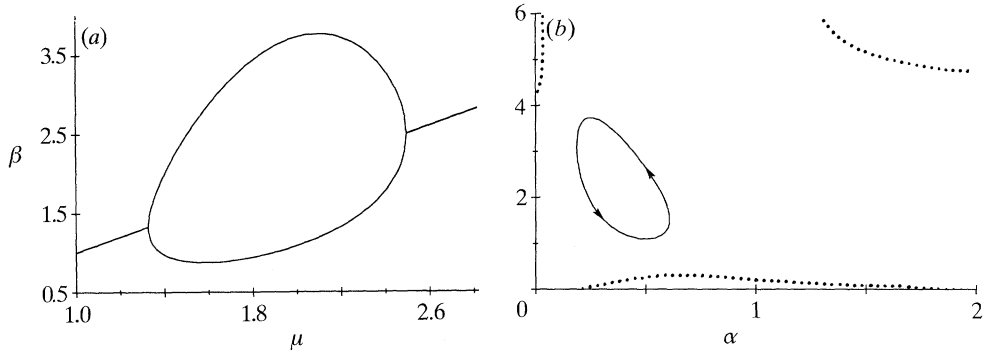

Figure 4. (*a*) Maximum and minimum of Autocatalator limit cycle oscillations as a function of bifurcation parameter μ with $\epsilon = 0.1$. Supercritical Hopf bifurcations occur at $\mu = 1.3281$ and 2.4972. (*b*) Phase plane showing the limit cycle (——) and inflection line (· · · ·) at $\mu = 2.0$, near the maximum amplitude of oscillations in β.

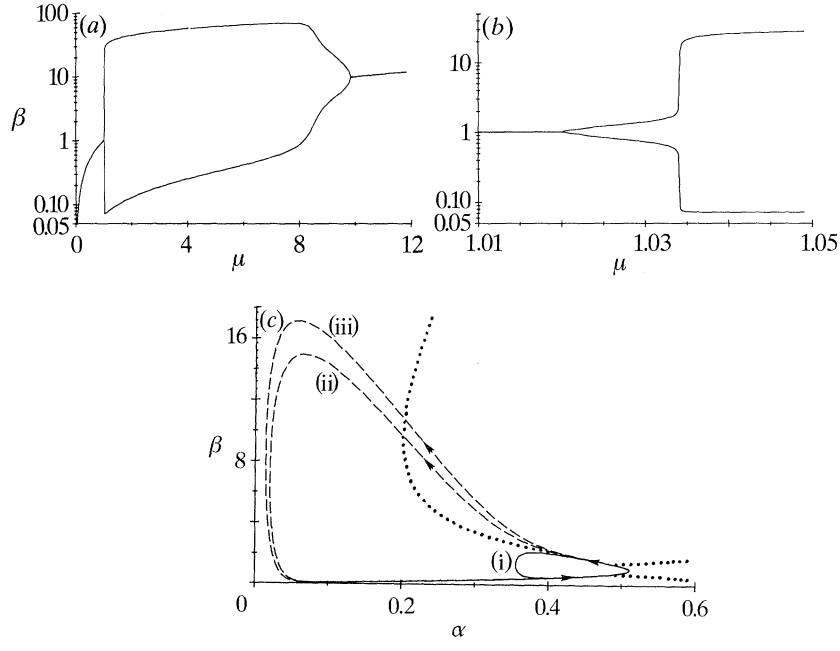

Figure 5. (*a*) Maximum and minimum of Autocatalator limit cycle oscillations as a function of bifurcation parameter μ with $\epsilon = 0.01$. Supercritical Hopf bifurcations occur at $\mu = 1.0206$ and 9.8467. (*b*) Enlargement of canard transition at $\mu \approx 1.034$. (*c*) Phase plane showing small-amplitude limit cycle (——, curve (i)) and large-amplitude limit cycles (– – –, curves (ii) and (iii)) immediately before and after the canard transition. Dotted curves show inflection line. Values of parameters: $\mu^{\mathrm{i}} = 1.0340$, $\mu^{\mathrm{ii}} = 1.0342$, $\mu^{\mathrm{iii}} = 1.0343$ and $\mu^{\mathrm{inf}} = 1.0341$.

concentrations of intermediates A and B, respectively, yields a two-variable system of differential equations:

$$\mathrm{d}\alpha/\mathrm{d}\tau = \mu - \alpha - \alpha\beta^2, \tag{B 1}$$

$$\epsilon\,\mathrm{d}\beta/\mathrm{d}\tau = \alpha + \alpha\beta^2 - \beta, \tag{B 2}$$

where $\epsilon = k_2/k_4$ and $\mu = (k_1/k_4)(k_3/k_2)^{\frac{1}{2}}P_0$ are dimensionless parameters.

Figure 4*a* shows steady-state and minimum and maximum values of β during limit

cycle oscillations as a function of μ for $\epsilon = 0.1$. The oscillations grow in a smooth, nearly parabolic manner to full amplitude from either of the supercritical Hopf bifurcations; canard behaviour is not observed for these parameter values. Shown in figure 4*b* are the limit cycle at $\mu = 2.0$, near the maximum oscillatory amplitude, and the corresponding inflection line (see Appendix B). It is clear that the inflection line lies far away from the limit cycle even at maximum amplitude. Because the limit cycle contracts on further increasing μ, a crossing of the inflection line cannot occur and canard behaviour is not exhibited.

In contrast, when $\epsilon = 0.01$, a sharp canard transition is exhibited at the lower limit of oscillations and moderate canard behaviour at the higher limit (figure 5*a*). A blow-up of the sharp canard is shown in figure 5*b*, and figure 5*c* shows the relative positions of the limit cycles and inflection line during the transition. The motion along the small limit cycle, which almost touches the inflection line, is counterclockwise. With a slight increase in μ, the trajectory crosses the line and large-amplitude oscillations appear (curves (ii) and (iii)). Unlike the previous example of the EOE system, however, κ_i and κ_t are of the same sign beyond the crossing point (case (*a*) in figure 3); therefore, the canard transition is continuous. It is likely that discontinuous transitions are also exhibited for some values of the parameters, although such behaviour was not found in this study.

6. Canard behaviour of unstable limit cycles in the two-variable Oregonator

The Oregonator was proposed by Field & Noyes (1974*a*, *b*) as a minimal model for the oscillatory Belousov–Zhabotinsky (BZ) reaction (Belousov 1959; Zhabotinsky 1964; Field & Burger 1985). The original three-variable scheme consists of five irreversible reactions:

$$\mathrm{A} + \mathrm{Y} \rightarrow \mathrm{X} + \mathrm{P}, \tag{6.1}$$

$$\mathrm{X} + \mathrm{Y} \rightarrow 2\mathrm{P}, \tag{6.2}$$

$$\mathrm{A} + \mathrm{X} \rightarrow 2\mathrm{X} + \mathrm{Z}, \tag{6.3}$$

$$2\mathrm{X} \rightarrow \mathrm{Q}, \tag{6.4}$$

$$\mathrm{Z} \rightarrow f\mathrm{Y}, \tag{6.5}$$

where the variables are $\mathrm{X} \equiv \mathrm{HBrO_2}$, $\mathrm{Y} \equiv \mathrm{Br^-}$ and $\mathrm{Z} \equiv \mathrm{Ce(IV)}$. The concentration of the reactant $\mathrm{A} \equiv \mathrm{BrO_3^-}$ is typically considered to be constant, and P and Q represent kinetically unimportant (in this model) oxybromine species such as HOBr. The parameter f is a stoichiometric factor relating the regeneration of Y to the consumption of Z. Introducing the dimensionless time $\tau = k_1 A t$ and the dimensionless variables $x = (k_2/k_1 A)X$, $y = (k_2/k_3 A)Y$ and $z = (k_2 k_5/k_1 k_3 A^2)Z$ for the concentrations of intermediates X, Y and Z yields a three-variable system of differential equations:

$$\sigma\, \mathrm{d}x/\mathrm{d}\tau = y - xy + x - \alpha x^2, \tag{C 1}$$

$$\mathrm{d}y/\mathrm{d}\tau = fz - y - xy, \tag{C 2}$$

$$\delta\, \mathrm{d}z/\mathrm{d}\tau = x - z, \tag{C 3}$$

where $\alpha = 2k_1 k_4/k_2 k_3$, $\delta = k_1 A/k_5$ and $\sigma = k_1/k_3$ are dimensionless parameters.

In reducing the model from three to two variables, we follow Bar-Eli & Noyes (1987), applying the original set of rate constants (Tyson 1977): $k_1 A = 0.2\ \mathrm{s^{-1}}$,

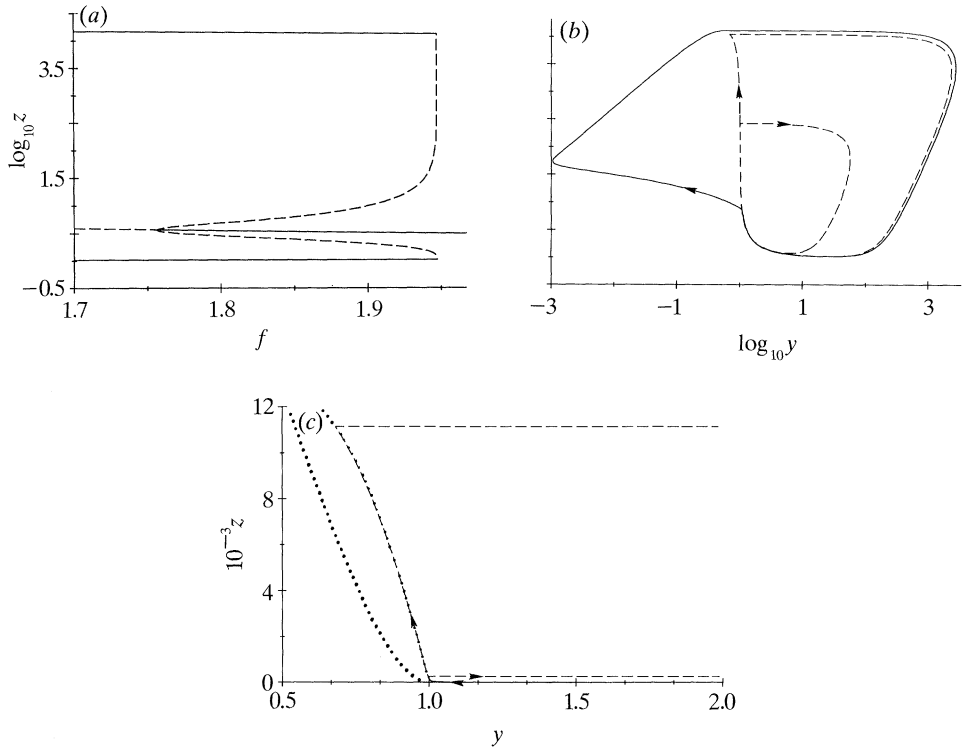

Figure 6. (*a*) Subcritical Hopf bifurcation in the Oregonator. Unstable steady state (– –) becomes stable and unstable limit cycle (– –) is formed, which grows until it touches the stable limit cycle (——). (*b*) Canard transition of the unstable limit cycle within the stable periodic orbit. For small-amplitude unstable limit cycle $f = 1.947$; for large-amplitude stable and unstable limit cycles and for the inflection line, $f = 1.947336$. (*c*) Blow-up of the lower region of phase plane shown in (*b*).

$k_2 = 2 \times 10^9$ M^{-1} s^{-1}, $k_3 A = 1 \times 10^3$ s^{-1}, $k_4 = 5 \times 10^7$ M^{-1} s^{-1} and $k_5 = 1$ s^{-1}. With these values, the dimensionless parameters α, δ and σ become 1×10^{-5}, 0.2 and 2×10^{-4} respectively. We utilize this reduction and these rate constants in order to connect with another study of canard behaviour in the Oregonator (Bar-Eli & Brons 1991). These parameter values permit the fast variable x to be expressed as a function of y:

$$x(y) = (1 - y + \sqrt{((1-y)^2 + 4\alpha y)})/2\alpha. \tag{C 4}$$

The two-variable reduction of the Oregonator provides a typical fast-slow dynamical system (Tyson 1977). For the parameter values used here, oscillatory behaviour both appears and disappears at subcritical Hopf bifurcations on varying the bifurcation parameter f (Bar-Eli & Noyes 1987). In a recent study, Bar-Eli & Brons (1991) examined canard behaviour occurring near a supercritical Hopf bifurcation, exhibited when the value of $k_1 A$ is increased to 1000. They located the stable and unstable manifolds in the phase plane and determined the value of the canard point in an analysis based on Diener's theory (1981, 1984) of canard behaviour in fast–slow systems.

The original rate constants are used here to investigate canard behaviour of an unstable limit cycle within a stable one, as shown in figure 6*a*. On increasing the value of f, the unstable focus is transformed at a subcritical Hopf bifurcation ($f^* \approx 1.755$) into a stable focus surrounded by an unstable limit cycle. The expanding

unstable limit cycle merges with the stable limit cycle; the confluence of the two limit cycles results in the disappearance of periodic solutions in a global bifurcation. The sharp increase in the amplitude of the unstable periodic solutions is a clear indication of a canard transition.

Figure 6*b* shows stable and unstable limit cycles near the onset of canard behaviour and subsequent confluence of the limit cycles. The unstable limit cycles in figure 6*a–c* were calculated by integrating the differential equations with time decreasing rather than increasing. A similar technique was used to characterize saddle-loop bifurcations of stable and unstable limit cycles in a two-variable Oregonator with flow terms (Gáspár & Showalter 1988; Gáspár *et al.* 1990).

The small unstable limit cycle approaches the inflection line (see Appendix C) from higher y values, as shown in the enlargement of the phase plane in figure 6*c*. Within the resolution shown in the figure, the crossing point seems to occur approximately midrange in the value of z. The curvature of the inflection line also seems to change sign in the same region; however, the calculations do not permit any conclusion concerning the continuity of the transition.

7. Canard behaviour in the van der Pol system

Canard behaviour was first investigated in the van der Pol oscillator (Diener 1981, 1984). Insights into the role of the inflection line can be gleaned from this non-chemical example. We examine here the same equations used in the earlier studies (Diener 1984; Kaas-Petersen & Brons 1985).

The van der Pol oscillator can be expressed as a second-order, ordinary differential equation:

$$\epsilon x'' + (x^2 - 1)\, x' + x - c = 0, \tag{D 1}$$

where x' and x'' denote the first and second derivatives with respect to time. Following Kaas-Petersen & Brons (1985) in casting (D 1) into a system of two first-order equations, we have

$$\epsilon\, \mathrm{d}x/\mathrm{d}t = (y - \tfrac{1}{3}x^3 + x), \tag{D 2}$$

$$\mathrm{d}y/\mathrm{d}t = c - x. \tag{D 3}$$

When ϵ is small, x is the fast variable and its nullcline constitutes the slow manifold of the system.

Figure 7*a* shows that when $\epsilon = 0.1$ small-amplitude oscillations develop at a supercritical Hopf bifurcation at $c^* = 1$. Harmonic oscillations are transformed into relaxation oscillations at the canard, occurring at $c \approx 0.986$. In figure 7*b* are shown the small and large limit cycles, immediately before and after the canard. As in the previous examples, the transition from small harmonic oscillations to large relaxation oscillations occurs when the limit cycle trajectory first touches and then crosses the inflection line (see Appendix D). For this value of ϵ, the canard transition is continuous since the configuration around the first crossing point corresponds to that shown in figure 3*a*.

For $\epsilon = 0.01$, the value used in earlier studies (Diener 1984; Kaas-Petersen & Brons 1985), the canard becomes much sharper (figure 7*c*). Because the limit cycle and inflection line take on opposite curvature after the crossing (see figure 3*b*), the canard behaviour is now discontinuous. The discontinuity explains why Diener *et al.* (1984) were unable to find any middle-sized oscillations even at their highest machine resolution.

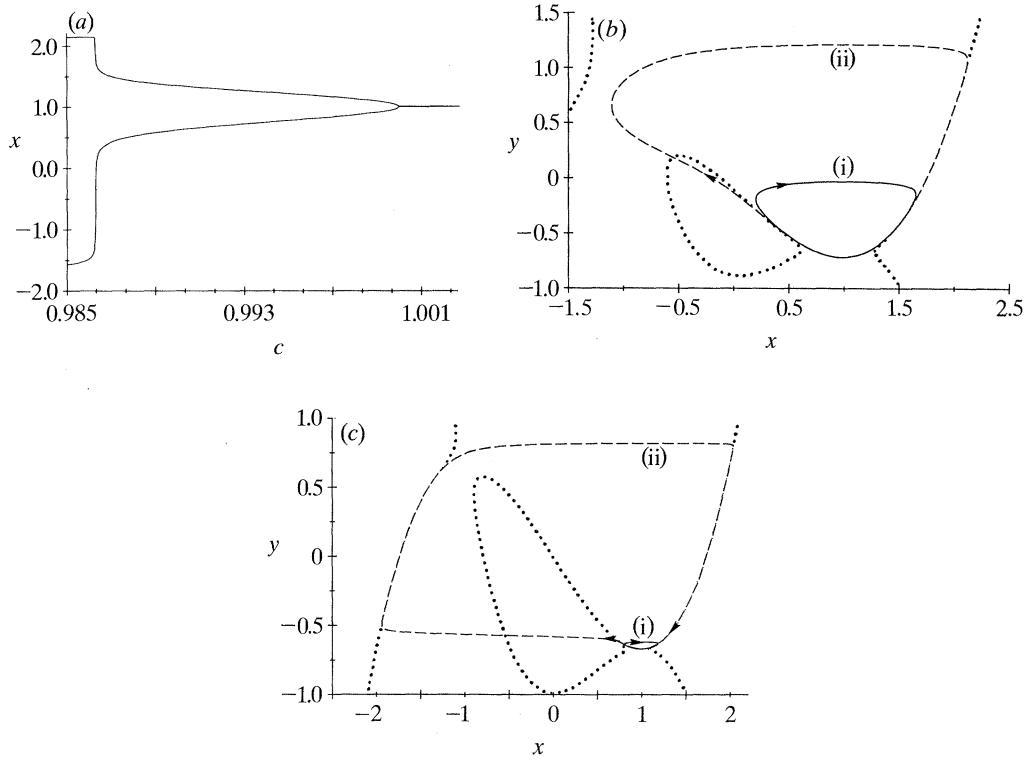

Figure 7. (*a*) Steady-state and maximum and minimum values of x as a function of bifurcation parameter c in the van der Pol system with $\epsilon = 0.1$. (*b*) Phase plane showing small-amplitude limit cycle (——, curve (i)) and large-amplitude limit cycle (- -, curve (ii)), calculated immediately before ($c^{\mathrm{i}} = 0.9864$) and after ($c^{\mathrm{ii}} = 0.9863$) the canard transition. Dotted curves show inflection line calculated at $c^{\mathrm{inf}} = c^{\mathrm{ii}}$. (*c*) Same as (*b*) but with $\epsilon = 0.01$. For curves (i) and (ii), $c^{\mathrm{i}} = 0.99875$ and $c^{\mathrm{ii}} = c^{\mathrm{inf}} = 0.99874$.

Figure 7*b*, *c* shows that additional crossings of the inflection line by the limit cycle trajectory do not result in dramatic changes in behaviour. The onset of canard behaviour always corresponds to a small limit cycle trajectory touching an inflection line tangentially; non-tangent crossings result only in mild changes of curvature.

8. Conclusion

An alternative approach of describing canard behaviour in terms of the inflection line in the phase plane provides insights into the transition of small-amplitude oscillations into large relaxation oscillations. The inflection line is the locus of points where the curvature of any of the possible phase plane trajectories is equal to zero. The onset of a canard transition occurs when a growing stable or unstable limit cycle trajectory tangentially touches an inflection line. The crossing coincides with a sharp change in the amplitude of oscillations. The curvature of the inflection line relative to that of the trajectory immediately following the crossing determines the continuity of a canard transition.

This work was supported by the National Science Foundation (Grants CHE-8920664 and INT-8822786) and NATO (Scientific Affairs Division, Grant 0124/89). We are grateful to the National Science Foundation and the Hungarian Academy of Sciences for support of a U.S.–Hungary

Cooperative Science Project. We thank K. Bar-Eli and M. Brons for sharing their results on canard behaviour before publication. We also thank S. K. Scott for valuable discussions. B.P. thanks the staff of the Department of Physical Chemistry and the Computer Center of Kossuth Lajos University for their friendly cooperation.

Appendix A. Two-variable model for the EOE reaction

The inflection line for the two-variable model of the oscillatory EOE reaction, equations (A 1)–(A 4), can be determined by the following expression:

$$\frac{\mathrm{d}^2Y}{\mathrm{d}X^2} =$$

$$\frac{-k_1(A\,\mathrm{d}Y/\mathrm{d}X + Y\,\mathrm{d}A/\mathrm{d}X) + k_{-1} + k_2 + 3k_4(Z + X\,\mathrm{d}Z/\mathrm{d}X) - 4k_3 Y\,\mathrm{d}Y/\mathrm{d}X - k_0\,\mathrm{d}Y/\mathrm{d}X}{k_1 AY - (k_{-1} + k_0 + k_2 + k_4 Z)X}$$

$$-[-k_1 AY + (k_{-1} + k_2 + 3k_4 Z)X - 2k_3 Y^2 + k_0(Y_0 - Y)]$$

$$\times [k_1(A\,\mathrm{d}Y/\mathrm{d}X + Y\,\mathrm{d}A/\mathrm{d}X) - (k_{-1} + k_0 + k_2) - k_4(Z + X\,\mathrm{d}Z/\mathrm{d}X)]$$

$$\times [k_1 AY - (k_{-1} + k_0 + k_2 + k_4 Z)X]^{-2} = 0, \tag{A 5}$$

where

$$\frac{\mathrm{d}Y}{\mathrm{d}X} = \frac{-k_1 AY + (k_{-1} + k_2 + 3k_4 Z)X - 2k_3 Y^2 + k_0(Y_0 - Y)}{k_1 AY - (k_{-1} + k_0 + k_2 + k_4 Z)X}, \tag{A 6}$$

$$\frac{\mathrm{d}A}{\mathrm{d}X} = \frac{k_{-1}(k_0 + k_1 Y) - k_1(k_0 A_0 + k_{-1} X)\,\mathrm{d}Y/\mathrm{d}X}{(k_0 + k_1 Y)^2}, \tag{A 7}$$

$$\frac{\mathrm{d}Z}{\mathrm{d}X} = \frac{2k_3 Y(k_0 + k_5 + k_4 X)\,\mathrm{d}Y/\mathrm{d}X - k_3 k_4 Y^2}{(k_0 + k_5 + k_4 X)^2}. \tag{A 8}$$

Appendix B. Autocatalator

The inflection line for the two-variable Autocatalator can be found by first constructing $\mathrm{d}\alpha/\mathrm{d}\beta$ from equations (B 1) and (B 2):

$$\frac{\mathrm{d}\alpha}{\mathrm{d}\beta} = \frac{\epsilon(\mu - \alpha - \alpha\beta^2)}{\alpha + \alpha\beta^2 - \beta}. \tag{B 3}$$

For $\mathrm{d}^2\alpha/\mathrm{d}\beta^2 = 0$, the second-order equation (B 4) is solved:

$$a\alpha^2 + b\alpha + c = 0, \tag{B 4}$$

where

$$a = (1 + \beta^2)(1 + 2\mu\beta - \beta^2), \tag{B 5a}$$

$$b = -(\mu - \beta)[2\beta^2 + \epsilon(1 + \beta^2)^2] - (\mu + \beta)(1 + \beta^2), \tag{B 5b}$$

$$c = \epsilon\mu(\mu - \beta)(1 + \beta^2) + \mu\beta. \tag{B 5c}$$

Appendix C. Oregonator

The inflection line for the two-variable Oregonator is given by

$$\frac{\mathrm{d}^2y}{\mathrm{d}z^2} = \frac{\delta}{(x - z)^2}\left[\left(f - \left(1 + x + y\frac{\mathrm{d}x}{\mathrm{d}y}\right)\frac{\mathrm{d}y}{\mathrm{d}z}\right)(x - z) - (fz - y - xy)\left(\frac{\mathrm{d}x}{\mathrm{d}y}\frac{\mathrm{d}y}{\mathrm{d}z} - 1\right)\right] = 0, \tag{C 5}$$

where dy/dz of (C 6) is obtained from (C 2) and (C 3),

$$\frac{dy}{dz} = \frac{\delta(fz-y-xy)}{x-z}, \tag{C 6}$$

and dx/dy of (C 7) is obtained from (C 4),

$$\frac{dx}{dy} = \frac{1-x}{\sqrt{((1-y)^2+4\alpha y)}}. \tag{C 7}$$

Appendix D. Van der Pol oscillator

The inflection line for the van der Pol oscillator can be determined by first obtaining dx/dy from (D 2) and (D 3):

$$\frac{dx}{dy} = \frac{y-\frac{1}{3}x^3+x}{\epsilon(c-x)}. \tag{D 4}$$

For $d^2x/dy^2 = 0$, the second-order equation (D 5) is solved:

$$y^2+ay+b = 0, \tag{D 5}$$

where

$$a = (1-x^2)(c-x)+2x(1-\tfrac{1}{3}x^2), \tag{D 6a}$$

$$b = \epsilon(c-x)^2+x(1-\tfrac{1}{3}x^2)[(1-x^2)(c-x)+x(1-\tfrac{1}{3}x^2)]. \tag{D 6b}$$

References

Andronov, A. A., Vitt, A. A. & Khaikin, S. E. 1966 *Theory of oscillators*. Oxford: Pergamon.

Bar-Eli, K. & Brons, M. 1991 *J. phys. Chem.* (In the press.)

Bar-Eli, K. & Noyes, R. M. 1987 *J. chem. Phys.* **86**, 1927–1937.

Belousov, B. P. 1959 *Ref. Radiat. Med.* **1958**, 145–147.

Benoit, E., Callot, J. L., Diener, F. & Diener, M. 1981 *Collect. Math.* **32**, 37–119.

Diener, M. & Poston, T. 1981 In *Chaos and order in nature* (ed. H. Haken), pp. 249–268. Berlin: Springer-Verlag.

Diener, M. 1984 *Math. Intell.* **6**, 38–49.

Edblom, E. C., Orbán, M. & Epstein, I. R. 1986 *J. Am. chem. Soc.* **108**, 2826–2830.

Field, R. J. & Burger, M. 1985 *Oscillations and traveling waves in chemical systems*. New York: Wiley.

Field, R. J. & Noyes, R. M. 1974*a* *J. chem. Phys.* **60**, 1877–1887.

Field, R. J. & Noyes, R. M. 1974*b* *Faraday Symp. Chem. Soc.* **9**, 21–27.

Gáspár, V. & Showalter, K. 1987 *J. Am. chem. Soc.* **109**, 4869–4876.

Gáspár, V. & Showalter, K. 1988 *J. chem. Phys.* **88**, 778–791.

Gáspár, V. & Showalter, K. 1990 *J. phys. Chem.* **94**, 4973–4979.

Gáspár, V., Peng, B. & Showalter, K. 1990 In *Spatial inhomogeneities and transient behaviour in chemical kinetics* (ed. P. Gray, G. Nicolis, F. Baras, P. Borckmans & S. K. Scott), pp. 279–289. Manchester University Press.

Gear, C. W. 1971 *Numerical initial value problems in ordinary differential equations*. Englewood Cliffs: Prentice-Hall.

Gray, B. F., Roberts, M. J. & Merkin, J. H. 1988 *J. Engng Math.* **22**, 267.

Gray, P. & Scott, S. K. 1986 *Ber. Bunsenges. Phys. Chem.* **90**, 985–996.

Hindmarsh, A. C. 1980 *Livermore solver of ordinary differential equations* (*LSODE*). Livermore, California: Lawrence Livermore Laboratory.

Kaas-Petersen, C. & Brons, M. 1985 In *Proc. 11th IMACS World Congress on Systematic Simulation and Scientific Computations*.

Korn, G. A. & Korn, T. M. 1961 *Mathematical handbook for scientists and engineers*, pp. 498–500. New York: McGraw-Hill.

Landolt, H. 1886 *Ber. Dtsch. Chem. Ges.* **19**, 1317–1365.

Merkin, J. H., Needham, D. J. & Scott, S. K. 1986 *Proc. R. Soc. Lond.* A **406**, 299–323.

Merkin, J. H., Needham, D. J. & Scott, S. K. 1987 *J. Engng Math.* **21**, 115–127.

Scott, S. K. & Tomlin, A. S. 1990 *Phil. Trans. R. Soc. Lond.* A **332**, 51–68.

Tyson, J. J. 1977 *J. chem. Phys.* **66**, 905–915.

Zhabotinsky, A. M. 1964 *Dokl. Akad. Nauk. SSSR* **157**, 392–395.